Proc. Natl. Acad. Sci. USA
Vol. 87, pp. 9108–9112, December 1990
Physiology/Pharmacology

Identification of a phenylalkylamine binding region within the α1 subunit of skeletal muscle Ca^{2+} channels

JÖRG STRIESSNIG*, HARTMUT GLOSSMANN†, AND WILLIAM A. CATTERALL*

*Department of Pharmacology, SJ-30, University of Washington, Seattle, WA 98195; and †Institute of Biochemical Pharmacology, Peter-Mayrstrasse 1, A-6020 Innsbruck, Austria

Contributed by William A. Catterall, August 23, 1990

ABSTRACT **The α1 subunit of the skeletal muscle Ca^{2+} channel has been specifically photoaffinity labeled with the phenylalkylamine-receptor-selective verapamil derivative (−)-5-{3-azidophenethyl[N-*methyl*-^{3}H]methylamino}-2-(3,4,5-trimethoxyphenyl)-2-isopropylvaleronitrile ([N-*methyl*-^{3}H]LU49888). Proteolytic fragments generated by various endoproteases were probed by immunoprecipitation with several sequence-specific antibodies to determine the site of labeling within the primary structure of α1. These results restrict the site of photolabeling by [N-*methyl*-^{3}H]LU49888 to the region between Glu-1349 and Trp-1391. This segment of α1 contains transmembrane helix S6 of domain IV and the beginning of the long intracellular C-terminal tail. Because the phenylalkylamine receptor site is only accessible from the intracellular side of the Ca^{2+} channel, we propose that the intracellular end of helix IVS6 and the adjacent intracellular amino acid residues play an essential role in formation of the phenylalkylamine receptor site. The action of the phenylalkylamines as open-channel blockers suggests that this region may also contribute to formation of the intracellular opening of the transmembrane pore of the Ca^{2+} channel.**

Voltage-dependent Ca^{2+} channels mediate the influx of Ca^{2+} ions into excitable cells upon membrane depolarization. At least four subtypes, termed P, T, N, and L type, can be distinguished by their biophysical and pharmacological properties (1). Only the L-type Ca^{2+} channels are modulated by distinct chemical classes of Ca^{2+} antagonists, such as phenylalkylamines (e.g., verapamil, desmethoxyverapamil, and gallopamil), 1,4-dihydropyridines (e.g., nifedipine, nitrendipine, and isradipine), or benzothiazepines [e.g., (+)-*cis*-diltiazem]. These drugs exert their effects by binding to distinct allosterically coupled drug receptors that have been shown to reside on the α1 subunit of the Ca^{2+} channel complex by photoaffinity labeling with receptor-selective probes (for review, see refs. 2–6). Functional studies suggest that the receptor for phenylalkylamine Ca^{2+}-channel blockers must be located intracellularly, because a quaternary membrane-impermeable verapamil derivative only blocks when applied to the intracellular side of the channel (7–9).

The primary structures of the rabbit skeletal muscle and heart α1 subunits derived from their cloned cDNA sequences (10, 11) reveal that these proteins are structurally homologous to the principal subunits of the voltage-gated Na^+ and K^+ channels and contain four internally homologous domains having six putative transmembrane segments, designated S1 through S6 (for review, see ref. 12). Although the primary structures of α1 subunits are now established, the regions that are involved in the formation of the drug receptors are unknown. Knowledge of the location of the drug binding domains within the channel-forming α1 subunit would help to clarify the molecular mechanisms of ion-channel gating, channel block, and allosteric drug effects. Here we define the localization of a phenylalkylamine-binding region within the α1 subunit of skeletal muscle Ca^{2+} channels by photoaffinity labeling with the phenylalkylamine-receptor-selective arylazide (−)-5-{3-azidophenethyl[N-*methyl*-^{3}H]methylamino}-2-(3,4,5-trimethoxyphenyl)-2-isopropylvaleronitrile ([N-*methyl*-^{3}H]LU49888) (13) and antibody mapping using a technique developed to localize the binding domain for α-scorpion toxin derivatives of Na^+ channels (14). Our results identify a region near the intracellular end of segment IVS6 as an important component of the phenylalkylamine receptor site.

EXPERIMENTAL PROCEDURES

Materials. [N-*methyl*-^{3}H]LU49888 (80 Ci/mmol; 1 Ci = 37 GBq) and (−)-desmethoxyverapamil were a gift from Knoll AG (Lugwigshafen, F.R.G.). L-1-Tosylamido-2-phenylethyl chloromethyl ketone-trypsin (from bovine pancreas) was obtained from Cooper Chemicals. V8 protease was from Boehringer Mannheim, Worthington, or Sigma. Soybean trypsin inhibitor was from Sigma and Affi-Gel 10 was from Bio-Rad. Prestained and unstained high and low molecular mass standards were obtained from BRL. EN^{3}HANCE, Protosol, and Econofluor were purchased from New England Nuclear. The sources of reagents used for Ca^{2+}-channel purification were described (15).

Photoaffinity Labeling of Partially Purified Ca^{2+} Channels. Ca^{2+} channels were solubilized in digitonin and purified by affinity chromatography on wheat germ agglutinin-Sepharose 4B, as described (15, 16). The pooled purified fractions (0.15 mg of protein per ml) were incubated with 30–60 nM [N-*methyl*-^{3}H]LU49888 for 45 min at 25°C. An aliquot of this mixture was incubated in the presence of 100 μM (−)-desmethoxyverapamil to determine nonspecific binding and photolabeling. The incubation mixtures were transferred into plastic Petri dishes on ice and dithiothreitol was added to a final concentration of 0.15 mM immediately before ultraviolet irradiation with a Sylvania germicidal lamp (10-cm distance, 2 min). After photolysis the samples were dialyzed against deionized water at room temperature for 5 hr, lyophilized, resuspended in 10 or 16% of the original volume, and stored at −25°C in small samples until use. This photolabeled sample contained specifically incorporated [N-*methyl*-^{3}H]LU49888 at 300–1600 cpm/μl, corresponding to labeling of 3–5% of the total α1 subunits. Nonspecific labeling was <5% of the total labeling as revealed by SDS/PAGE. No other polypeptide present in the partially purified Ca^{2+}-channel preparation was labeled by [N-*methyl*-^{3}H]LU49888.

Reductive Carboxymethylation of [N-*methyl*-^{3}H]LU49888-Labeled α1 Subunits. Dialyzed photolabeled sample was reduced for 30 min at room temperature with 1% 2-mercap-

The publication costs of this article were defrayed in part by page charge payment. This article must therefore be hereby marked "*advertisement*" in accordance with 18 U.S.C. §1734 solely to indicate this fact.

Abbreviation: [N-*methyl*-^{3}H]LU49888, (−)-5-{3-azidophenethyl[N-*methyl*-^{3}H]methylamino}-2-(3,4,5-trimethoxyphenyl)-2-isopropylvaleronitrile.

toethanol in the presence of 1.6% (wt/vol) SDS and 150 mM Tris Cl (pH 8.4). Iodoacetamide was then added from a freshly prepared aqueous stock solution to a final concentration of 70 mM. After incubation for 45 min, the reagents and SDS were removed by dialysis against 6 M urea, as described (10). The sample was lyophilized and stored at −25°C until use.

Proteolysis of [N-*methyl*-^{3}H]LU49888-Labeled α1 Subunits. Digitonin-solubilized native [N-*methyl*-^{3}H]LU49888-α1 subunits were digested with trypsin by adding 1 vol of dialyzed [N-*methyl*-^{3}H]LU49888-α1 to 2.6 vol of distilled water and 0.4 vol of trypsin solution in 0.1 mM Tris Cl (pH 8.3), followed by incubation at 37°C for 120 min. The conditions for proteolysis of denatured [N-*methyl*-^{3}H]LU49888-α1 subunits with trypsin, endoproteinase Lys-C, and V8 protease are given in the figure legends. The reactions were stopped by the addition of SDS sample buffer except for immunoprecipitation experiments in which the mixtures were boiled for 3 min in 0.7–1.0% SDS (or 2–4 M urea). The samples were then adjusted to 1% Triton X-100, 0.1% SDS (or 0.2–0.4 M urea), bovine serum albumin (0.5–1.0 mg/ml), trypsin inhibitor (for trypsin) (0.5–1 mg/ml), 150 mM NaCl, and 25 mM Tris Cl (pH 7.4).

Immunoprecipitation. Antibodies were bound to protein A-Sepharose 4B by incubating 1 vol of serum with 1 vol of swollen gel in RIA buffer containing 25 mM Tris Cl (pH 7.4), 150 mM NaCl, 1% Triton X-100, and bovine serum albumin (0.5 mg/ml) for 15 min at 4°C. The gel was washed with RIA buffer before the addition of digested or nondigested [N-*methyl*-^{3}H]LU49888-α1 prepared as described above. After incubation for 90–120 min at 25°C, the gel pellets were washed with RIA buffer and processed for SDS/PAGE (see below) or resuspended in 6% SDS for determination of antibody-bound radioactivity by liquid scintillation counting.

SDS/PAGE, Gel-Slicing, and Autoradiography. Standard SDS/PAGE was carried out according to Laemmli (gel system 1, 5–20% or 10–20% polyacrylamide gradients; gel system 2, 16% polyacrylamide). For separation of smaller fragments in the 3- to 20-kDa range, the gel system described by Schaegger and von Jagow (17) was used (gel system 3: stacking gel, 4% T, 3% C; spacer gel, 10% T, 3% C; separating gel, 16.5% T, 6% C, where T is total monomer and C is crosslinker). Prestained molecular mass standards were used to generate standard curves from which the apparent molecular mass of the peptides of interest was calculated by nonlinear regression analysis. Lysozyme migrated abnormally fast in gel systems 2 and 3 and was, therefore, omitted from the standard curves. To determine protein-bound radioactivity, gels were fixed or stained with Coomassie blue R-250, impregnated with EN^{3}HANCE, and processed for fluorography, according to the manufacturers' instructions. Gels containing a high concentration of acrylamide often cracked under these processing conditions, but the resolution of labeled peptide bands was not significantly impaired. Alternatively, individual gel lanes were manually cut into 4-mm slices and radioactivity was eluted in 3% (vol/vol) Protosol in Econofluor (13).

Site-Directed Antibodies. The generation of polyclonal antisera against peptides corresponding to residues 687–700 [CP-(687–700)], 1082–1099 [CP-(1082–1099)], and 1505–1522 [CP-(1505–1522)] was described (18). Additional antisera were produced against peptides corresponding to residues 743–759 [CP-(743–759)], 1339–1354 [CP-(1339–1354)], and 1382–1400 [CP-(1382–1400)]. IgG fractions were isolated by chromatography on protein A-Sepharose. Anti-CP-(1382–1400) antibodies were affinity purified by passing antiserum over a 1.5-ml column of CP-(1382–1400) covalently attached to Affi-Gel 10. Elution was achieved with 0.5 M NaCl/0.2 M acetic acid. The eluate was neutralized immediately with Tris base and stored at −25°C in small samples until use.

RESULTS AND DISCUSSION

Isolation of a 9.5-kDa Fragment Specifically Photolabeled with [N-*methyl*-^{3}H]LU49888. Fig. 1*A* shows an SDS/PAGE analysis of the partially purified specifically photolabeled α1 subunit (lane 1). No radioactivity was detected by fluorography in samples where the phenylalkylamine receptor was protected by an excess of the unlabeled competitive blocker (−)-desmethoxyverapamil (lanes 2, 4, 6, 8, and 10). Treatment of the nondenatured digitonin-solubilized sample with increasing trypsin concentrations for 120 min at 37°C produced a well-defined series of photolabeled peptide fragments (lanes 3, 5, 7, and 9). Digestion with trypsin (1 μg/ml) reproducibly generated a major 30-kDa fragment and, in most experiments, an additional 57-kDa/63-kDa doublet. Quantification of the radioactivity from gel slices revealed that 30–52% and 0–20% (range, n = 3 to 6) of the applied radioactivity was present in these fragments, respectively. Trypsin (10–100 μg/ml) produced a fragment migrating faster than the 18-kDa standard in gel system 1 (lanes 7 and 9). A molecular mass of 9.5 ± 0.2 kDa (n = 5; mean ± SD) was determined after better resolution in gel systems 2 and 3 (Fig. 1*B*). This fragment contained 55–65% (range, n = 4) of the total α1-associated radioactivity; no other radioactive labeled protein bands were detected. A time course (0–120 min) of proteolysis with an intermediate enzyme concentration (3 μg/ml) revealed the progressive appearance of the 9.5-kDa polypeptide concomitant with the time-dependent breakdown of the 57/63- and 30-kDa fragments (data not shown). This suggests that most of the specific labeling occurs within a region of 9.5 kDa in the α1 subunit and that the 57/63-kDa and 30-kDa fragments are precursors to the 9.5-kDa fragment in the proteolytic digestion.

The 9.5-kDa Fragment Binds to Antibodies Directed Against Intracellular and Extracellular Segments Adjacent to IVS6. To determine their localization within the primary structure, we first probed these photolabeled tryptic fragments by immunoprecipitation with several site-directed antibodies raised against different intracellular portions of the α1 subunit. Photolabeled subunits were digested with different concentrations of trypsin and then immunoprecipitated with the site-directed antibodies against peptides CP-(687–700), CP-(743–759), CP-(1082–1099), CP-(1382–1400), and CP-(1505–1522) (Fig. 2).

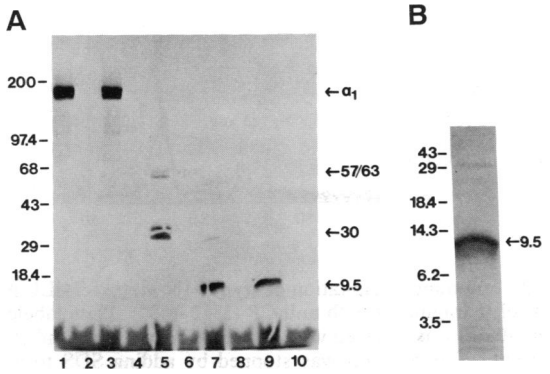

FIG. 1. Limited tryptic digestion of the nondenatured [N-*methyl*-^{3}H]LU49888-photolabeled α1 subunit. (*A*) α1 subunit (15 μg) photolabeled in the absence (lanes 1, 3, 5, 7, and 9) or presence (lanes 2, 4, 6, 8, and 10) of 100 μM (−)-desmethoxyverapamil was digested with trypsin at 0 (lanes 1 and 2), 0.1 (lanes 3 and 4), 1 (lanes 5 and 6), 10 (lanes 7 and 8), and 100 (lanes 9 and 10) μg/ml at 37°C for 120 min. The reaction was stopped by addition of boiling sample buffer and separation of the peptides in gel system 1 (5–20% polyacrylamide) followed by fluorography of the dried gel. The migration of the molecular mass standards (molecular mass in kDa) is indicated to the left. (*B*) Digestion was as for lane 9 of *A*, but separation was carried out in a minigel apparatus using gel system 3.

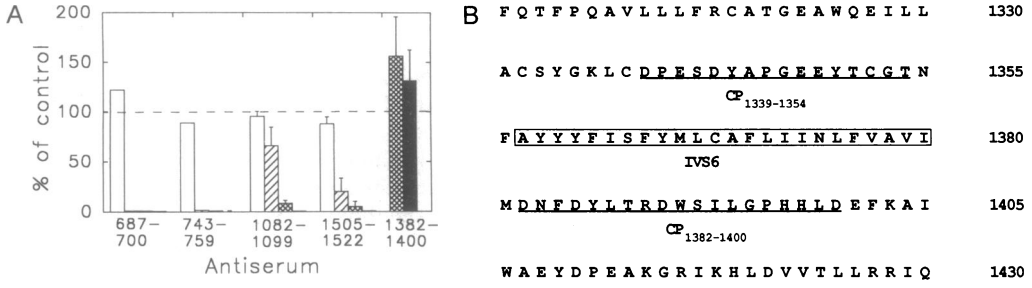

FIG. 2. Immunoprecipitation of tryptic fragments of the [N-*methyl*-^{3}H]LU49888-photolabeled α1 subunit by various site-directed antibodies. (*A*) Photolabeled α1 subunit was digested with trypsin at 0 (100%, control), 0.3 (open bars), 1 (hatched bars), 10 (cross-hatched bars), and 100 (solid bars) μg/ml and immunoprecipitated with antiserum directed against the peptides indicated. The radioactivity bound to the protein A-Sepharose-adsorbed antibody was determined, after elution from the pellet in 6% SDS, by liquid scintillation counting. The data are expressed as the percent of precipitation compared with the control sample. Data from several experiments using antisera collected from rabbits at different times and different photolabeled Ca^{2+}-channel preparations were pooled. Data are given as mean ± SD for $n > 2$. (*B*) Amino acid sequence near segment IVS6. Boxed sequence is IVS6; underlined sequences are CP-(1339–1354) and CP-(1382–1400).

The amount of radioactivity bound by anti-CP-(687–700), anti-CP-(743–759), anti-CP-(1082–1099), and anti-CP-(1505–1522) progressively decreased with increasing enzyme concentrations suggesting that their binding sites are separated from the [N-*methyl*-^{3}H]LU49888 incorporation site upon proteolysis. None of these antibodies immunoprecipitated radioactivity under conditions where only the 9.5-kDa fragment was present (trypsin at 10–100 μg/ml). In contrast, the amount of α1-bound [N-*methyl*-^{3}H]LU49888 immunoprecipitated by anti-CP-(1382–1400), which is directed against the first 19 amino acids at the intracellular end of segment IVS6 (see Fig. 2*B* for location of this sequence), increased upon proteolytic treatment. These results indicate that the site of covalent labeling is located near the CP-(1382–1400) segment and becomes more accessible for antibody binding after tryptic cleavage. The binding of the antibodies was specific as no radioactivity was precipitated by nonimmune sera or when sera were preincubated with an excess of the corresponding peptides. CP-(1382–1400) inhibited the binding of photolabeled α1 to anti-CP-(1382–1400) with an IC_{50} value of 10–20 nM whereas 100 nM of CP-(743–759) was without effect.

SDS/PAGE analysis of the photolabeled peptides that were immunoprecipitated by anti-CP-(1382–1400) is shown in Fig. 3. [N-*methyl*-^{3}H]LU49888-labeled α1 was digested with trypsin at 1 μg/ml (Fig. 3*A*) or 100 μg/ml (Fig. 3*B*) and equivalent amounts of sample were loaded on the gel directly or after immunoprecipitation with anti-CP-(1382–1400). As expected, the photolabeled proteolytic fragments of 30 kDa and 9.5 kDa were both recognized by the antibody, confirming the localization of the site of covalent labeling to the 9.5-kDa fragment.

To define the position of the 9.5-kDa fragment in the primary structure of the α1 subunit more precisely, antibodies were produced that recognize CP-(1339–1354), the segment immediately at the extracellular end of IVS6 (Fig. 2*B*). After digestion of the labeled α1 subunit with trypsin (100 μg/ml), anti-CP-(1339–1354) immunoprecipitated 60% of the radioactivity associated with α1 subunits whereas control antibodies were ineffective (Fig. 4 *Inset*). Analysis of the

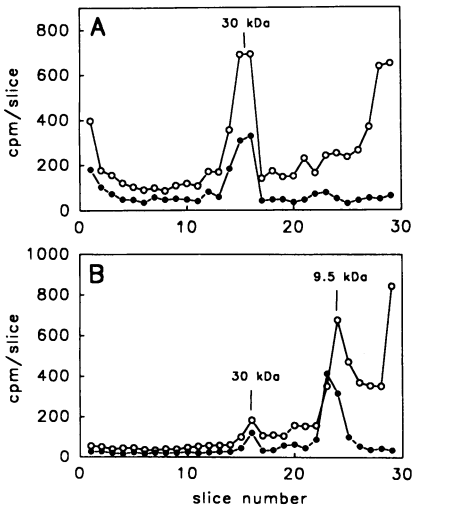

FIG. 3. Immunoprecipitation of tryptic [N-*methyl*-^{3}H]LU49888-photolabeled fragments with anti-CP-(1382–1400). Photolabeled α1 subunit (30 μg) was digested with trypsin at 1 and 100 μg/ml at 37°C for 120 min. The reaction was stopped by adding SDS to a final concentration of 0.7% and boiling for 3 min. Half of the mixture was immunoprecipitated (solid circles) with anti-CP-(1382–1400) IgG (equivalent to 50 μl of antiserum) (*A*) or affinity-purified antibody (*B*). After separation of the total sample (open circles) and immunoprecipitated sample (solid circles) in gel system 1 (10–20% polyacrylamide), individual lanes were cut into 4-mm slices and extracted with 3% (vol/vol) Protosol in Econofluor. Radioactivity was determined by liquid scintillation counting with a counting efficiency of 30%. Prestained molecular mass standards were applied to parallel lanes and used to calculate the apparent molecular mass of the fragments. Note that the background of nonimmunoprecipitated samples increases toward the dye front where the bulk of radioactivity incorporated into low molecular mass components migrates.

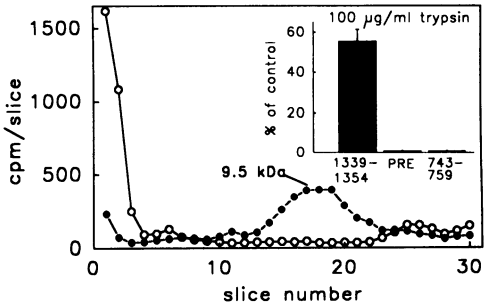

FIG. 4. Immunoprecipitation of [N-*methyl*-^{3}H]LU49888-photolabeled α1 and tryptic fragments with anti-CP-(1339–1354). Photolabeled α1 subunit (20 μg) was digested with trypsin at 0 (open circles) and 100 (solid circles) μg/ml and immunoprecipitated with anti-CP-(1339–1354) immunoglobulin (equivalent to 0.2 ml of antiserum) and the samples were separated in gel system 3 and radioactivity was measured as described in Fig. 3. Note that the nondigested α1 migrated at the top of the gel in this system. The digested peak was broader in the immunoprecipitated samples because of the high amount of antibody loaded. (*Inset*) After immunoprecipitation with anti-peptide antibodies or preimmune serum (PRE), the antibody-bound radioactivity was determined directly by liquid scintillation counting. Data were normalized with respect to the nondigested control immunoprecipitated with anti-CP-(1339–1354). Data from four experiments were pooled and given as mean ± SD, $n = 4$.

precipitates by SDS/PAGE using gel system 3 showed that anti-CP-(1339–1354) immunoprecipitated the 9.5-kDa photolabeled peptide. Approximately 60% of the specifically incorporated photolabel was recovered in the immunoprecipitated 9.5-kDa fragment, in good agreement with the relative amount of radioactivity associated with the 9.5-kDa fragment (Fig. 4). These results indicate that this antibody recognizes intact and digested α1 subunits with similar efficiency.

Inspection of the potential tryptic cleavage sites (arginine and lysine residues) in this region of the α1 subunit (see amino acid sequence in Fig. 2*B*) reveals that the N terminus of the 9.5-kDa tryptic fragment containing CP-(1382–1400) and CP-(1339–1354) sequences must result from cleavage at Lys-1336 or Arg-1318 and its C terminus from cleavage at Lys-1403, Lys-1414, Lys-1418, or Arg-1416. This peptide fragment contains the S6 α-helical segment of domain IV of the Ca^{2+} channel α1 subunit and adjacent extracellular and cytoplasmic sequences.

Isolation and Characterization of Smaller Photolabeled Fragments. To generate smaller proteolytic fragments, digestion was carried out for a longer period of time (24 hr at 37°C) after complete denaturation of the protein. Under these conditions, the smallest fragment produced by trypsin (Fig. 5*A*, lane 1) was 8.4 ± 0.3 kDa (mean ± SD, n = 6), indistinguishable in size from a fragment of 8.2 ± 0.2 kDa (n = 4) produced by the lysine-specific endoproteinase Lys-C (Fig. 5*B*, lanes 1 and 3). As this fragment was immunoprecipitated by anti-CP-(1382–1400) (Fig. 5 *A*, lane 2, and *B*, lanes 2 and 4), its N terminus must arise from cleavage at Lys-1336 and its C terminus at Lys-1403 (calculated molecular mass, 7.9 kDa) or possibly Lys-1414 (calculated molecular mass, 9.2 kDa).

Smaller fragments could be generated by treatment of the fully denatured photolabeled preparation at 37°C for 24 hr with V8 protease, which cleaves at glutamic acid and aspartic acid residues. Fig. 5*A* (lanes 3–6) shows that labeled peptides with apparent molecular masses of 6.3, 5.9, and 4.8 kDa were obtained in various experiments. Even the smallest peptide fragment was immunoprecipitated by anti-CP-(1382–1400) (lanes 5 and 6). Similar sized fragments were observed when the 9.5-kDa tryptic fragment was affinity purified with anti-CP-(1382–1400) and then further digested with V8 protease (data not shown), indicating that the V8 fragments are contained within the 9.5-kDa peptide. Inspection of the amino acid sequence between Lys-1336 and Lys-1418 (see Fig. 2*B*) shows that the N termini of the 6.3- and 5.9-kDa fragments must be located on the extracellular side of IVS6 and the C termini on the intracellular side to account for their size. Considering its size, its immunoprecipitation by anti-CP-(1382–1400) (Fig. 5*A*, lanes 3 and 5), and its lack of immunoprecipitation by anti-CP-(1339–1354), the 4.8-kDa fragment produced by complete digestion likely results from cleavage at Glu-1349 to yield the N terminus and at Asp-1390 to yield the C terminus (calculated molecular mass, 4.9 kDa). This fragment contains nine residues of CP-(1382–1400) sequence, which would likely be sufficient for antibody recognition. Evidently, cleavages at Asp-1382 and Asp-1385 are prevented by their proximity to transmembrane segment IVS6.

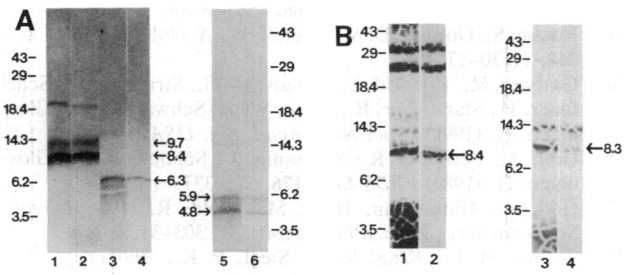

FIG. 5. Proteolysis of denatured [N-*methyl*-^{3}H]LU49888-photolabeled α1 subunit with trypsin, V8-protease, or endoproteinase Lys-C. (*A*) The photolabeled preparation was reductively carboxymethylated and lyophilized after removal of SDS by dialysis against urea and water. Labeled α1 subunit (150 μg) was resuspended in 50 mM ammonium bicarbonate (pH 8.6) or 40 mM sodium phosphate (pH 7.8) and digested at 37°C for 24 hr with trypsin (300 μg/ml, lanes 1 and 2) or V8 protease (400–500 international units/ml, lanes 3–6), respectively. SDS at 0.1% was added to the incubations corresponding to lanes 5 and 6. The tryptic digest (60%) and the V8 digest (50%) were then immunoprecipitated with anti-CP-(1382–1400) (lanes 2, 4, and 6) corresponding to 50 μl of antiserum and separated side by side with the nonimmunoprecipitated samples (lanes 1, 3, and 5). (*B*) Reductively carboxymethylated channel (150 μg, lanes 1 and 2) or nontreated photolabeled α1 (20 μg) was digested with endoproteinase Lys-C (4 units/ml) for 24 hr at 37°C in the presence of 2 M urea. Separation, in gel system C, was followed by fluorography of the dried gel. The migration of molecular mass standards (given as kDa) is indicated.

Properties of the Site of Photolabeling. The peptide fragments that we have characterized account for the majority of the [N-*methyl*-^{3}H]LU49888 specifically photoincorporated into the α1 subunit (55–65%). It is possible that photolabeling occurs at additional minor sites or on phospholipid and contributes to the 35–45% not characterized in this work. However, it is very unlikely that sites other than those in close proximity to the ligand binding site are specifically photolabeled. Our photolabeling was done on ice to minimize dissociation. In addition, we added dithiothreitol before initiating photolysis as a thiol scavenger to destroy photogenerated intermediates formed outside of or dissociating from the binding site. These precautions, along with the high specificity of the photolabeling reaction (Fig. 1), strongly support the conclusion that the site of covalent labeling that we have identified is a major component of the phenylalkylamine receptor site.

Our results restrict the site of photolabeling by [N-*methyl*-^{3}H]LU49888 to the region between Glu-1349 and Trp-1391. This sequence contains seven extracellular residues, segment IVS6 itself, and nine intracellular residues at the beginning of the C-terminal tail of the α1 subunit. The corresponding S6 segment of domain 1 of the Na^+ channel has been shown definitively to be a transmembrane segment because components of the receptor site for α-scorpion toxins are located at its extracellular end (14) and confirmed sites of cAMP-dependent protein phosphorylation in intact neurons are located at its intracellular end (19). Since the transmembrane folding of the homologous domains is expected to be identical for all voltage-gated ion channels, it is very likely that segment IVS6 of the calcium channel α1 subunit is also a transmembrane segment. Thus, the phenylalkylamine receptor site is in or near a transmembrane segment of the α1 subunit.

The amino acid sequence of IVS6 and the first third of the C-terminal tail is highly conserved among the α1 subunits so far fully sequenced (rabbit and carp skeletal muscle and rabbit cardiac muscle; refs. 7, 8, and 20). The reversible binding properties of phenylalkylamines to these channel subunits and the modulation of their binding by divalent cations (3, 13, 21–23) are almost identical, suggesting that a highly conserved motif must be involved in the formation of the phenylalkylamine receptor. Phenylalkylamines contain a tertiary amine nitrogen with a pK value of ≈8.5 and are active as cations (24). As the positively charged tertiary amino nitrogen is an essential component for high-affinity binding of phenylalkylamines, negatively charged residues are expected to be present in the drug receptor site. Inspection of the intracellular portion of the [N-*methyl*-^{3}H]LU49888-labeled region reveals three negatively charged aspartic acid residues at positions 1382, 1385, and 1390 (Fig. 2*B*), which are conserved in each of the known sequences of α1 subunits.

One or more of these negatively charged residues may participate directly in the binding of phenylalkylamines or negatively charged residues from a more distant intracellular segment may fold to form the receptor site.

Formation of the Transmembrane Pore in Voltage-Gated Ion Channels. The primary structures of Ca^{2+} channel $\alpha 1$ subunits establish that they are members of the voltage-gated ion-channel gene family that also includes the voltage-gated Na^+ and K^+ channels. Despite considerable progress in defining the structure–function relationships of the voltage-gated ion channels, no accepted structural model for formation of a transmembrane pore by this family of proteins has emerged. All six putative transmembrane segments (S1 through S6) have been proposed to form the lining of the transmembrane pore in one or more models of channel structure (for review, see ref. 12). Direct information on the segments of the voltage-gated channels that form their transmembrane pores may be derived from studies that localize the receptor sites for drugs having a channel-blocking action. Acidic amino acid residues that are important for high-affinity binding of ligands to the receptor sites for tetrodotoxin and charybdotoxin, extracellular blockers of Na^+ and K^+ channels, respectively, have been identified in the peptide segments on the extracellular side of transmembrane segment S6 by site-directed mutagenesis (25–27). These results suggest that protein segments on the extracellular side of S6 may form the extracellular entry to the transmembrane pore of Na^+ and K^+ channels.

The frequency-dependent block of Ca^{2+} channels by phenylalkylamines resembles the block of Na^+ channels by tertiary and quaternary local anesthetics (28). Therefore, as proposed for local anesthetic block of Na^+ channels, phenylalkylamines may bind within the intracellular opening of the transmembrane pore of the ion channel and may reach their binding site by a hydrophilic pathway from the intracellular side. This model is supported by studies with D-890, a permanently charged membrane-impermeant derivative of verapamil that only blocks Ca^{2+} channels when administered from the cytoplasmic side (7–9). Since the phenylalkylamines behave as open-channel blockers acting from the intracellular side of the channel, our results indicate that the intracellular opening of the transmembrane pore may be formed by the cytoplasmic end of transmembrane segments S6 and the adjacent intracellular residues. Indeed, we speculate that Asp-1382 and Asp-1385, which would be located on adjacent turns on the same side of an α-helix, may play a critical role in both binding of phenylalkylamines and in coordination of calcium ions entering and exiting from the transmembrane pore on the cytoplasmic side. Calcium binding to this region of the $\alpha 1$ subunit is also suggested by the presence of an EF hand calcium-binding motif in the amino acid sequence (29). Thus, our present results and previous work (14, 25–27) on Na^+ and K^+ channels indicate that protein segments adjacent to S6 transmembrane segments form the extracellular and intracellular openings of the transmembrane pore and suggest the surprising hypothesis that the hydrophobic, but highly conserved, S6 segments of the voltage-gated ion channels may in fact form part or all of the walls of the transmembrane pore. Further work to test this idea will be important in defining the structure and function of this family of ion-channel proteins.

We thank Dr. Karen DeJongh and Mr. Ruti Clark for help in peptide synthesis, Ms. Santosh Kumar for help in amino acid analysis, and Dr. Joseph Beavo for critical comments on the manuscript. This work was supported by Miles Laboratories, by Research Grant NS22625 from the National Institutes of Health to W.A.C. and by grants from the Fonds zur Förderung der Wissenschaftlichen Forschung and the Ostereichische Nationalbank to H.G. J.S. is a recipient of a postdoctoral research fellowship from the Max Kade Foundation Inc.

1. Hess, P. (1990) *Annu. Rev. Neurosci.* **13,** 337–356.
2. Catterall, W. A., Seagar, M. J. & Takahashi, M. (1988) *J. Biol. Chem.* **263,** 3535–3538.
3. Glossmann, H. & Striessnig, J. (1990) *Rev. Physiol. Biochem. Pharmacol.* **114,** 1–105.
4. Campbell, K. P., Leung, A. T. & Sharp, A. H. (1988) *Trends Neurosci.* **11,** 425–430.
5. Hofmann, F., Nastainczyk, W., Röehrkasten, A., Schneider, T. & Sieber, M. (1987) *Trends Pharmacol. Sci.* **8,** 393–398.
6. Hosey, M. M. & Lazdunski, M. (1988) *J. Membr. Biol.* **104,** 81–106.
7. Hescheler, J., Pelzer, D., Trube, G. & Trautwein, W. (1982) *Pflügers Arch.* **393,** 287–291.
8. Affolter, H. & Coronado, R. (1986) *Biophys. J.* **49,** 767–771.
9. Valdivia, H. H. & Coronado, R. (1989) *J. Gen. Physiol.* **95,** 1–27.
10. Tanabe, T., Takeshima, H., Mikami, A., Flockerzi, V., Takahashi, H., Kangawa, K., Kojima, M., Matsuo, H., Hirose, T. & Numa, S. (1987) *Nature (London)* **328,** 313–318.
11. Mikami, A., Imoto, K., Tanabe, T., Niidome, T., Mori, Y., Takeshima, H., Narumiya, S. & Numa, S. (1989) *Nature (London)* **340,** 230–233.
12. Catterall, W. A. (1988) *Science* **242,** 50–61.
13. Striessnig, J., Knaus, H. G., Grabner, M., Moosburger, K., Seitz, W., Lietz, H. & Glossmann, H. (1987) *FEBS Lett.* **212,** 247–253.
14. Tejedor, F. J. & Catterall, W. A. (1988) *Proc. Natl. Acad. Sci. USA* **85,** 8742–8746.
15. Curtis, B. M. & Catterall, W. A. (1984) *Biochemistry* **23,** 2113–2118.
16. Striessnig, J. & Glossmann, H. (1991) *Methods Neurosci.*, in press.
17. Schaegger, H. & von Jagow, G. (1987) *Anal. Biochem.* **166,** 368–379.
18. De Jongh, K. S., Merrick, D. K. & Catterall, W. A. (1989) *Proc. Natl. Acad. Sci. USA* **86,** 8585–8589.
19. Rossie, S., Gordon, D. & Catterall, W. A. (1987) *J. Biol. Chem.* **262,** 17530–17535.
20. Grabner, M., Friedrid, U., Knaus, H.-G., Striessnig, J., Scheffauer, F., Standinger, R., Koch, W. J., Schwartz, A. & Glossmann, H. (1991) *Proc. Natl. Acad. Sci. USA*, in press.
21. Goll, A., Ferry, D. R., Striessnig, J., Schober, M. & Glossmann, H. (1984) *FEBS Lett.* **176,** 371–377.
22. Goll, A., Glossmann, H. & Mannhold, R. (1986) *Naunyn Schmiedebergs Arch. Pharmacol.* **334,** 303–312.
23. Garcia, M. L., King, V. F., Siegl, P. K., Reuben, J. P. & Kaczorowski, G. J. (1986) *J. Biol. Chem.* **261,** 8146–8157.
24. Rodenkirchen, R., Bayer, R. & Mannhold, R. (1982) *Prog. Pharmacol.* **5,** 9–23.
25. Noda M., Suzuki, H., Numa, S. & Stühmer, W. (1989) *FEBS Lett.* **259,** 213–216.
26. MacKinnon, R. & Miller, C. (1989) *Science* **145,** 1382–1385.
27. MacKinnon, R. (1990) *Biophys. J.* **57,** 209 (abstr.).
28. Hille, B. (1984) *Ionic Channels in Excitable Membranes* (Sinauer, Sunderland, MA).
29. Babitch, J. (1990) *Nature* **346,** 321–322.